AGU PUBLICATIONS

Global Biogeochemical Cycles

RESEARCH ARTICLE
10.1002/2016GB005528

Avoidable impacts of ocean warming on marine primary production: Insights from the CESM ensembles

Kristen M. Krumhardt[1], Nicole S. Lovenduski[2], Matthew C. Long[3], and Keith Lindsay[3]

[1]Environmental Studies Program and Institute of Arctic and Alpine Research, University of Colorado Boulder, Boulder, Colorado, USA, [2]Department of Atmospheric and Oceanic Sciences and Institute of Arctic and Alpine Research, University of Colorado Boulder, Boulder, Colorado, USA, [3]Climate and Global Dynamics Laboratory, National Center for Atmospheric Research, Boulder, Colorado, USA

Key Points:
- Climate warming during the 21st century results in reduced marine net primary production on a global scale
- Ensemble simulations allow for an investigation of ensemble mean trends across two emission scenarios in the presence of natural variability
- Significant decreases in marine net primary production in the Atlantic basin may be avoided with a mitigation emission scenario

Supporting Information:
- Supporting Information S1
- Figure S1
- Figure S2
- Figure S3
- Figure S4

Correspondence to:
K. M. Krumhardt,
kristen.krumhardt@colorado.edu

Citation:
Krumhardt, K. M., N. S. Lovenduski, M. C. Long, and K. Lindsay (2017), Avoidable impacts of ocean warming on marine primary production: Insights from the CESM ensembles, *Global Biogeochem. Cycles*, *31*, 114–133, doi:10.1002/2016GB005528.

Received 12 SEP 2016
Accepted 12 DEC 2016
Accepted article online 16 DEC 2016
Published online 24 JAN 2017

©2016. American Geophysical Union. All Rights Reserved.

Abstract As anthropogenic emissions and warming continue to alter Earth's environment, it is essential to highlight future impacts that can be avoided through mitigation. Here we use two ensembles of the Community Earth System Model (CESM) run under the business-as-usual scenario, RCP 8.5, and the mitigation scenario, RCP 4.5, to identify avoidable impacts of anthropogenic warming on marine net primary production (NPP). We emphasize the use of ensembles so as to distinguish long-term, anthropogenic trends in marine productivity from internal variability. Twentieth century globally integrated marine NPP is 55.7 ± 1 Pg C, with much of the variability attributable to certain regions (e.g., the equatorial Pacific). CESM projections indicate that global marine NPP will drop by ~4% by 2080 if we follow RCP 8.5, but only by 2% under RCP 4.5. The response to warming on a global scale includes compensating regional effects; NPP increases in polar and eastern equatorial Pacific waters but decreases in the Atlantic, western Pacific, and Indian Oceans. The two main phytoplankton groups simulated in CESM show distinct responses: diatoms decrease their NPP, while small phytoplankton NPP increases over the mid-21st century. Trends in NPP from mid-21st century to 2080 are significantly different between the two emission scenarios mainly in the Atlantic Ocean basin and therefore impacts here are "avoidable" if we follow RCP 4.5, rather than RCP 8.5. In contrast, changes in NPP on a global scale and in most areas of the Pacific and Indian basins and the Southern Ocean are not distinguishable between forcing scenarios.

1. Introduction

Marine phytoplankton are responsible for roughly half of the primary production on Earth, making them an influential force on the global carbon cycle [*Falkowski*, 2012]. Changes in the marine environment resulting from anthropogenic carbon emissions and warming may lead to alterations in phytoplankton growth and species distribution [*Pörtner et al.*, 2014]. This, in turn, could cause reorganizations of — and productivity shifts within — marine biomes. Comprising the base of the marine food web, how phytoplankton respond to climate change will have cascading effects throughout marine ecosystems, ultimately affecting living marine resources, such as fishery yields [*Cheung et al.*, 2010; *Pörtner et al.*, 2014].

The timing and magnitude of marine environmental changes in nutrient availability, temperature, and light, which control phytoplankton productivity, are ultimately influenced by the rate of anthropogenic emissions (and associated warming) in the future. Emissions stabilize mid-21st century under the mitigation scenario RCP 4.5, while current rates of emissions continue under RCP 8.5. This concept has been applied in the Benefits of Reduced Anthropogenic Climate changE experiments [*Sanderson et al.*, 2015], which have examined various avoidable 21st century impacts of climate change on, e.g., crop yields [*Levis et al.*, 2016] or temperature extremes [*Tebaldi and Wehner*, 2016]. Though significant increases in surface temperature can be avoided with carbon emission mitigation, more complex ecosystem characteristics, such as marine NPP, may show less distinction between emission scenarios since they integrate both the direct (i.e., temperature) and indirect consequences of global warming (e.g., changes in circulation, shifts in nutrient, or light availability). Examining where significant differences exist between RCP 4.5 and RCP 8.5 is critical for demonstrating the benefits of mitigation, as well as focusing adaptation costs.

Earth system models included in the Coupled Model Intercomparison Project Phase 5 (CMIP5) show consistent decreases in globally integrated marine NPP by 2100, though the magnitude of the decrease varies

substantially from model to model [*Bopp et al.*, 2013; *Cabré et al.*, 2015]. Even when forced with a common emission scenario, CMIP5 models exhibit a large spread in NPP projections by 2100 (ranging from −2% to −30% under RCP 8.5) [*Bopp et al.*, 2013; *Cabré et al.*, 2015], driven by differences in both model structure and internal variability (e.g., El Niño–Southern Oscillation and North Atlantic Oscillation). Model structural differences that could contribute to this range in NPP projections arise from differing structures of the underlying ocean circulation and atmospheric models, the complexity of the ecosystem model, and the parameterization of biogeochemical processes [*Laufkötter et al.*, 2015]. A model's internal variability can also contribute to uncertainty in future NPP projections, especially on regional scales [*Frölicher et al.*, 2016].

Coupled Earth system models develop their own realizations of internal climate variability. While the characteristic timescale, magnitude, and spatial pattern of particular modes of variability are consistent between identically forced simulations, the phasing of natural variability is sensitive to minute differences in initial conditions and can influence climate projections, especially on short timescales [*Hawkins and Sutton*, 2009]. Therefore, an effective way to distinguish internal variability from forced trends in ocean biogeochemistry is through an ensemble of simulations, which differ only slightly in initial conditions [*Frölicher et al.*, 2009; *Rodgers et al.*, 2015; *Long et al.*, 2016; *McKinley et al.*, 2016; *Lovenduski et al.*, 2016; *Frölicher et al.*, 2016]. While ensemble members represent individual realizations of Earth's climate, the ensemble mean demonstrates forced trends [*Deser et al.*, 2012].

In order to quantify avoidable changes in marine NPP, we employ two ensemble integrations of CESM: the large ensemble, forced with a business-as-usual carbon emission scenario (RCP 8.5) [*Kay et al.*, 2015], and the medium ensemble, forced with a mitigation scenario (RCP 4.5) [*Sanderson et al.*, 2015]. Differences between the ensemble means of these two experiments can be used to quantify the impact of differences in the forcing scenario on trends in marine NPP. While *Moore et al.* [2013] evaluate predicted changes to ecosystem structure and biogeochemistry in CESM under RCP 4.5 and RCP 8.5, our study is unique because (1) we quantify internal variability in order to show where NPP changes under RCP 4.5 and 8.5 are statistically different, (2) we examine the response of regional phytoplankton dynamics to these changing oceanic conditions, and (3) we identify avoidable marine NPP impacts in the CESM ensembles using ecologically relevant regions (marine biomes—see section 2).

We first evaluate CESM's internal variability and trends in marine NPP (section 2), followed by an analysis of avoidable marine NPP impacts on global to regional scales. Climate warming drives decreased productivity in tropical and subtropical regions, and, although productivity increases in some high-latitude biomes, there is an overall decrease in global NPP. We demonstrate how the two main types of phytoplankton simulated in CESM (small phytoplankton and diatoms) alter their growth rates in response to anthropogenic warming: decreases in diatom production are somewhat offset by increasing NPP by small phytoplankton. Many regions of the ocean show mid-21st century trends in NPP that are not significantly different between forcing scenarios RCP 8.5 and RCP 4.5; however, we show that NPP differences in the Atlantic Ocean are significant and therefore can be considered avoidable. As we will show, circulation in the Atlantic is particularly sensitive to the effects of warming in CESM, leading to larger decreases in marine NPP under RCP 8.5. These results help to clarify impacts of possible future warming on marine ecosystems, highlighting where mitigation may help avoid some adverse effects of anthropogenic climate change during the latter half of the 21st century.

2. Materials and Methods

2.1. Model Description

The CESM large ensemble (CESM-LE) and CESM medium ensemble (CESM-ME) simulations are described in detail in *Kay et al.* [2015] and *Sanderson et al.* [2015], respectively. Briefly, the Community Earth System Model version 1 (CESM1), with ocean, land, sea ice, and biogeochemistry components, was run at a nominal 1° resolution. The CESM ensembles began as a 1500 year preindustrial control simulation run until Earth's climate was in quasi-equilibrium. Ensemble member 1 was then started from initial conditions in a randomly selected year of the control run and integrated forward from 1850 to 2100 under historical and then RCP 8.5 forcing. All other CESM-LE members were started from the 1920 state of ensemble member 1 with small (10^{-14}°C) changes in the air temperature field. The CESM-ME simulations, which are forced with the RCP 4.5 emission scenario, were branched off from the first 15 CESM-LE members at 2006 and run until 2080. Unfortunately, six CESM-LE/ME members had corrupted ocean biogeochemistry, and therefore, for this study we use the 34 CESM-LE members and nine CESM-ME members that have valid ocean biogeochemistry. Further details about

the simulations, as well as validation of ocean carbon fluxes from CESM-LE/ME can be found in *Lovenduski et al.* [2016] and *McKinley et al.* [2016].

The CESM ocean biogeochemistry component includes three phytoplankton functional types (PFTs): small phytoplankton, diatoms, and diazotrophs [*Moore et al.*, 2004, 2013; *Long et al.*, 2013]. Each PFT has a unique fundamental role in marine ecosystems. The small phytoplankton fare better in warmer, low-nutrient environments, while diatoms possess fast intrinsic growth rates in cooler, high-nutrient environments. This is represented in the model parameterization by smaller half-saturation constants for nutrient uptake by small phytoplankton, while diatoms have the ability to more efficiently photoadapt under high-nutrient conditions. Diazotrophs can fix atmospheric nitrogen (N) and therefore are not limited by N availability, unlike the two other PFTs. In CESM, each PFT has a maximum growth rate, which is attenuated by temperature, nutrient, and light availability [*Moore et al.*, 2004, 2013]. Climatic warming can cause changes in each of these factors, influencing phytoplankton growth, which, in turn, can alter phytoplankton assemblages and total NPP. Most directly, PFT growth rates are scaled by a temperature function with a Q10 of 2.0 and reference temperature of 30°C. Apart from these bottom-up influences, top-down controls, such as zooplankton grazing, can also affect phytoplankton biomass and productivity. Grazing rates increase with temperature, and small phytoplankton have moderately higher grazing pressure than diatoms.

2.2. Statistical Methods

Analyses were conducted on annual mean output corrected for model drift by subtracting a linear trend computed from the 1500 year preindustrial control integration of ensemble member 1 (described above) from all ensemble member simulations over the period corresponding to 1920–2100. Vertical integrals of primary productivity from each PFT were calculated, then summed to create global maps of net marine primary production. We use decadal averages of the ensemble means to compute NPP difference maps so as to minimize any residual internal variability.

We classified the oceanic environment into seven major biomes as in *Sarmiento et al.* [2004], which are formulated based on latitude (which indirectly incorporates the influence of light supply) and annual mean physical ocean characteristics affecting nutrient availability, specifically mixed layer depth, vertical velocity at 50 m, and ice fraction. Equatorial biomes reside between 5°S and 5°N and are separated into upwelling (Eq-U) and downwelling regions (Eq-D; determined by the sign of the vertical velocity at 50 m of depth). The low-latitude upwelling biome (LL-U), defined by positive vertical velocity at 50 m of depth between the latitudes 30°N and south of 35°S (excluding the equatorial biomes), is primarily around the western margins of continents and generally shows high productivity. In contrast, the subtropical permanently stratified biome (ST-PS) is characterized by downwelling and low productivity, as mixed layer depths never exceed 150 m. A subtropical seasonally stratified biome (ST-SS) has similar characteristics, but with mixed layer depths deepening past 150 m during the winter. Subpolar biomes (SP) are defined as upwelling regions north of 30°N or south of 35°S. Southern subpolar biome areas are less productive than their northern counterpart due to iron limitation [*Sarmiento et al.*, 2004]. Lastly, the marginal sea ice biome (ICE) is the region covered by sea ice for any part of the year.

To describe avoidable impacts in detail, we divided up the world ocean by hemisphere (North or South), biome boundaries in the year 2049, and major basin (Pacific, Indian, or Atlantic). We used biome boundaries for 2049, the beginning year of our NPP linear regressions (see next paragraph), because the boundaries do not differ greatly between RCP scenarios until after this year. This process yields 40 regions (2 hemispheres $\times$7 biomes $\times$3 major basins = 42; 42 − 2 nonexistent regions = 40; the Northern Hemisphere Indian basin does not have subpolar and marginal sea ice biomes).

Since the CESM-ME simulations ended at 2080, we end our marine NPP comparison between RCP 4.5 and 8.5 at this year. Though the purpose of this study is to show future marine NPP impacts that can be avoided through mitigation, we also verified that global mean marine NPP during the historic period (1920 to 1951) is significantly higher than average marine NPP from 2049 to 2080 under both forcing scenarios (Figure S1). Thus, some impacts from anthropogenic warming appear to be unavoidable on a global level regardless of whether RCP 4.5 or 8.5 is followed. Nevertheless, to assess future avoidable impacts with mitigation (RCP 4.5), we fit a least squares regression line to total NPP and NPP from each PFT from 2049 to 2080, the most divergent period between the two emission scenarios in terms of total NPP, to assess avoidable impacts. This time period encompasses 32 years of data, reported to be the global mean time series length necessary to observe long-term changes in marine primary productivity [*Henson et al.*, 2016]. Within each CESM ensemble, there

is variability in NPP trends over this period among ensemble members due to internal variability. Therefore, in order to demonstrate the spread of NPP trends among ensemble members and show probability density of NPP trends in a given region, trends for each ensemble member from 2049 to 2080 were binned by 0.002 g C m^{-2} yr^{-2} intervals. In order to assess whether NPP trends in each region were "avoidable" or not, we used a 1σ confidence interval (68.3%)—if confidence intervals in NPP trends between the two emission scenario ensembles did not overlap, then significant 21st century warming impacts were deemed as avoidable. Large internal variability in a certain region will contribute to more overlap of NPP trends between ensemble members from the RCP 4.5 and 8.5 scenarios.

2.3. Evaluating Model Marine NPP Variability

We used primary production estimates from the Hawaiian Ocean Time-series (HOT) and the Bermuda Atlantic Time-series Study (BATS), as well as global, satellite-derived NPP to evaluate internal variability of CESM simulated NPP. NPP data from the Moderate Resolution Imaging Spectroradiometer (MODIS; 2003 to 2015) was generated using the standard Vertically Generalized Production Model (VGPM). The VGPM calculates NPP based on chlorophyll, available light, and photosynthetic efficiency [*Behrenfeld and Falkowski*, 1997]. Data from 12 h light bottle incubations performed at the HOT and BATS sites were filtered using a 1 year boxcar filter and used to examine annual variability in NPP at these study site locations (Figure 1). We used satellite-derived NPP from the grid cells encompassing BATS and HOT sites, annually averaged and interpolated onto a 1° grid, to evaluate marine NPP variability at these locations (shown in Figures 1a and 1b in red).

Mean CESM NPP is within the range outlined by the site data and the satellite observations, but interannual variability is substantially higher in the in situ observations. The standard deviation of primary production is 15.9 g C m^{-2} yr^{-1} at HOT and 33.7 g C m^{-2} yr^{-1} at BATS, while standard deviation in CESM grid cells corresponding to these sites over an overlapping time period are ~3 g C m^{-2} yr^{-1} and ~7 g C m^{-2} yr^{-1}, respectively. We suggest that this discrepancy is partly due to the coarse spatial resolution of the model (~1°), which omits important scales of variability, including mesoscale eddies. This is supported by the similarity in NPP standard deviation between CESM-LE members and the satellite data interpolated onto a 1° grid (Figure S2). The model captures lower NPP variability in the subtropical North Pacific relative to the subtropical North Atlantic (Figure 1), consistent with the in situ and satellite data. CESM simulations show that these two subtropical locations have comparably low NPP variability relative to other regions, such as the equatorial regions of the Pacific and Indian Oceans, as well as areas of the Southern Ocean (Figure 1c). A full comparison of NPP standard deviation from 2003 to 2015 between all CESM-LE members and the satellite data is presented in Figure S3. Overall patterns of standard deviation in marine NPP match between the model and the data. However, CESM tends to underestimate marine NPP variability in coastal regions and in the far North Pacific and North Atlantic, while overestimating marine NPP variability in the equatorial Pacific and Indian Oceans (though satellite observations from 2003 to 2015 lack a significant El Niño event; Figure S3).

We compare trends in marine NPP over the MODIS satellite period (2003–2015) with two ensemble members to demonstrate the large role of internal variability over this short time period (Figure 2; see Figure S4 for a comparison to all ensemble members). Figure 2b shows an ensemble member with a pattern in NPP trends similar to that of the satellite record, decreasing NPP in the eastern equatorial Pacific and increasing NPP in the eastern subtropical Atlantic. An alternative view of NPP trends are seen for the ensemble member shown in Figure 2c. Neither of these ensemble members capture the observed NPP increases in the subpolar North Atlantic (though others do; Figure S4), but both show spotty NPP increases in the Southern Ocean, as in the observations (Figure 2). While forced trends (i.e., the ensemble mean; Figure 2d) are not directly comparable to the satellite record (which comprise forced, long-term trends + internal variability), we do see positive trends in NPP in high latitudes, consistent with the satellite record. As following sections will demonstrate, it is this large internal variability that complicates our ability to detect avoidable impacts in marine NPP.

3. Results

3.1. Global Overview

Global mean marine NPP drops from 55.7 Pg C yr^{-1} to 53.7 Pg C yr^{-1} from 1920 to 2080 in the CESM ensemble mean under RCP 8.5, a decline of 3.6% (Figure 3). In contrast, ensemble members forced under the RCP 4.5 scenario show less decline in globally integrated NPP, with the ensemble mean NPP in the ocean reaching 54.6 Pg C yr^{-1} by 2080, which is roughly half of the decline simulated under RCP 8.5 (Figure 3a). The impact of climate variability on simulated global NPP is substantial, indicated by an ensemble spread that is generally

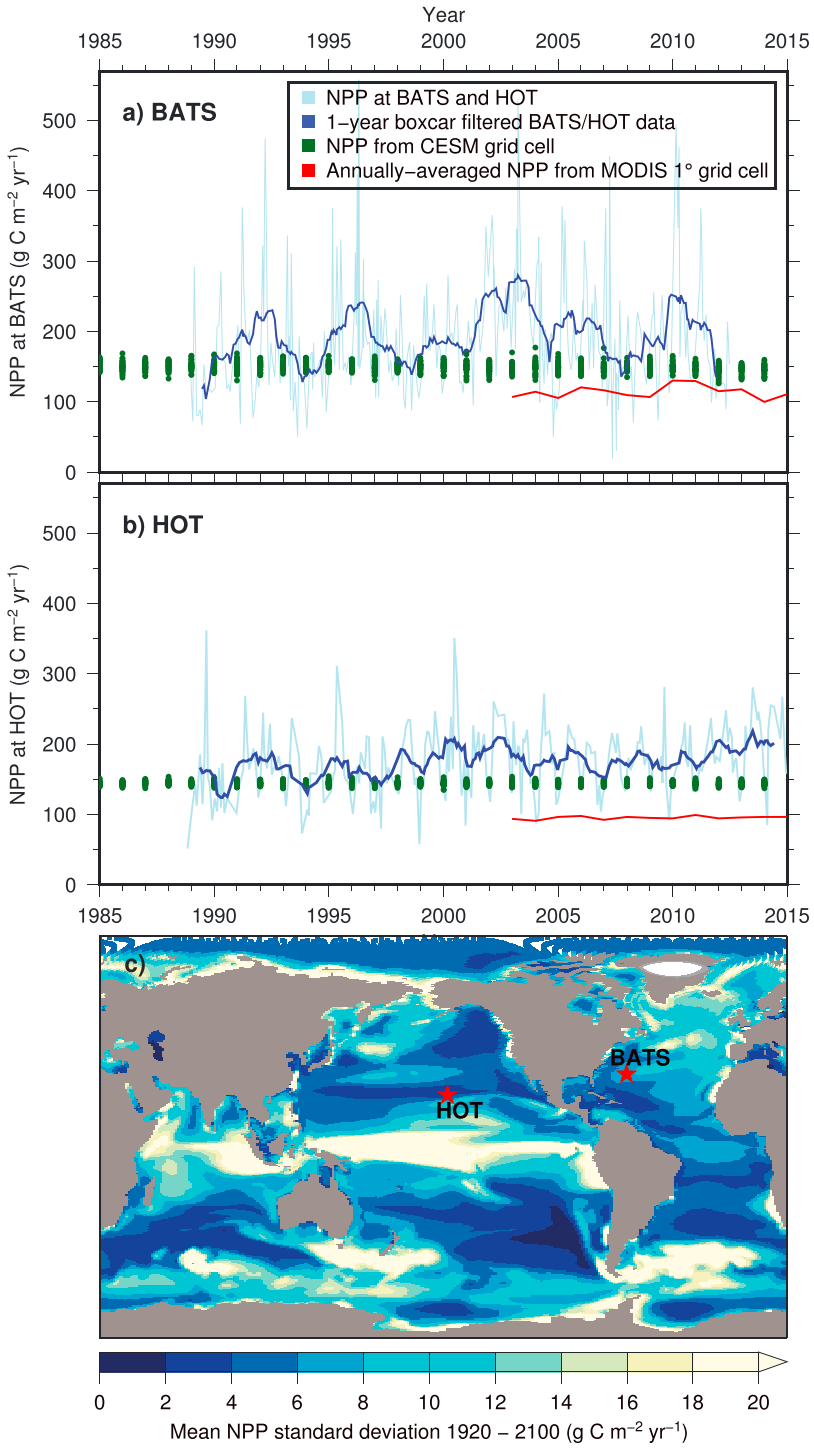

Figure 1. Primary productivity observations from study sites (a) BATS in the subtropical North Atlantic and (b) HOT in the subtropical North Pacific and (c) global average standard deviation in annual NPP among ensemble members from the CESM-LE simulations (1920–2100). Primary production at BATS and HOT was estimated using 12 h light bottle carbon fixation integrated over the euphotic zone using trapezoidal Riemann approximations. Light blue lines are the original data, while darker blue lines show a 1 year boxcar filter on the data (annual mean primary production). MODIS satellite-derived data (interpolated to 1° grid and annually averaged) is presented in red for the grid cells encompassing BATS and HOT sites. For comparison, depth-integrated NPP from CESM in the grid cell encompassing each site are shown for each ensemble member in green (the spread shows variation among ensemble members). Global average standard deviation in annual NPP (Figure 1c) was calculated by computing the standard deviation across ensemble members for each year and then taking the mean standard deviation over time (1920–2100).

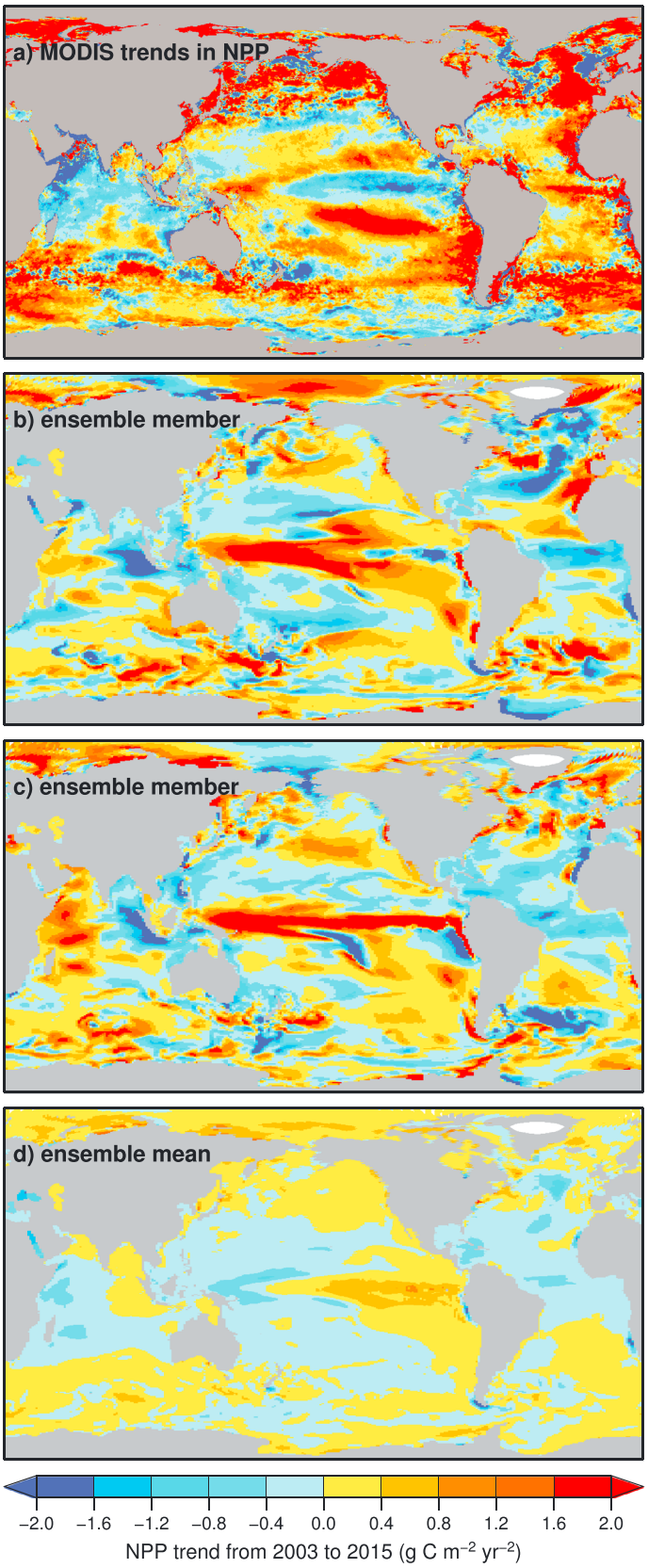

Figure 2. Trends in net primary production from 2003 to 2015 from (a) MODIS satellite data using VGPM model, (b) ensemble member 103, (c) ensemble member 014, and (d) the ensemble mean.

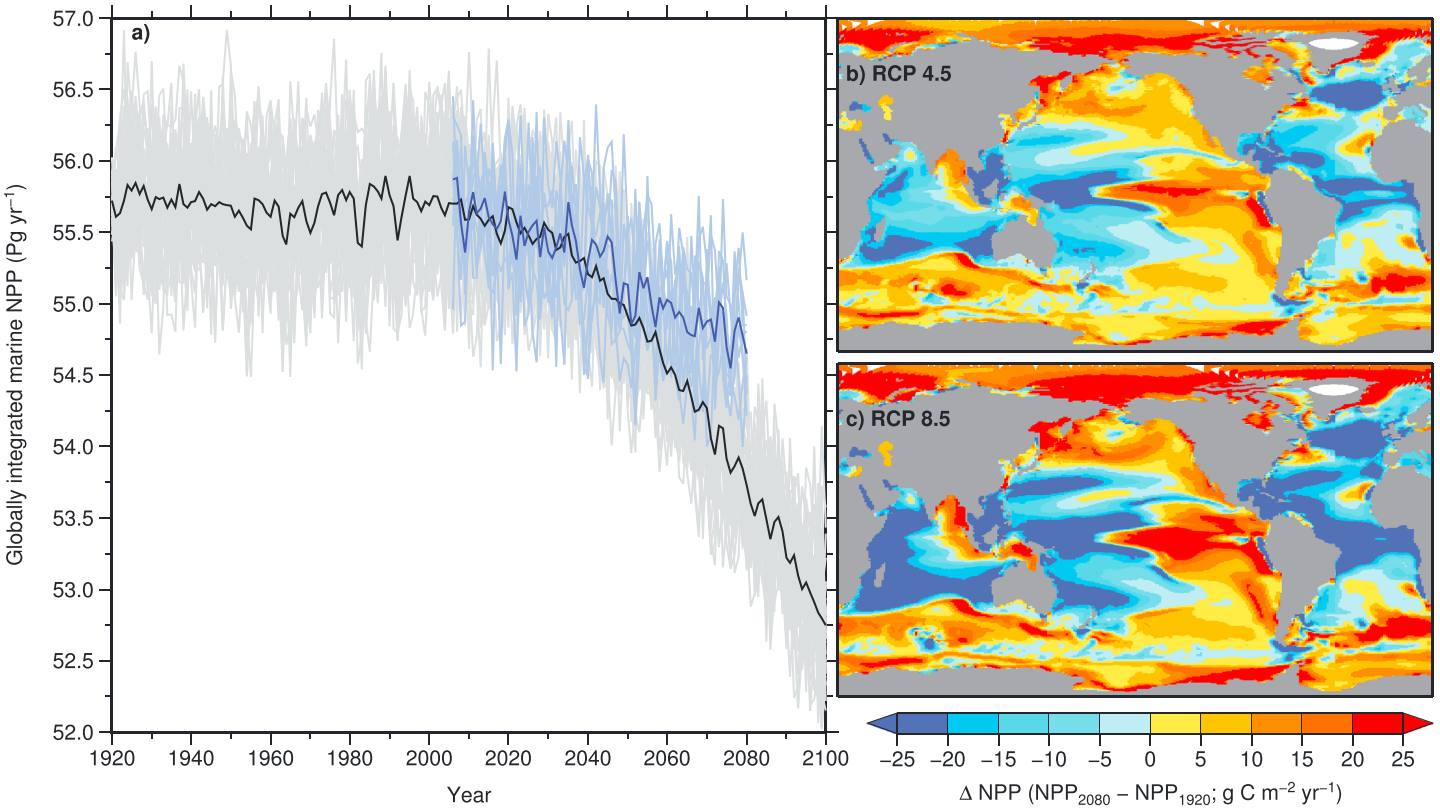

Figure 3. A comparison of global changes in marine NPP from 1920 to 2080. (a) Globally integrated NPP from the CESM ensembles for RCP 4.5 (ensemble mean in blue, ensemble members in light blue) and RCP 8.5 (ensemble mean in black, ensemble members in gray). The change in ensemble mean marine NPP from 1920 to 2080 for (b) RCP 4.5 and (c) RCP 8.5 using decadal averages (1920–1929 and 2071–2080).

between 1 and 2 Pg C yr^{-1} (σ = 0.36 Pg C yr^{-1} for CESM-LE 1920–2100) and fairly consistent in time and between forcing scenarios (Figure 3a). Due to large variability there is substantial overlap between projections under the two emission scenarios, making it difficult to distinguish between them. On this basis, we find that global declines in NPP cannot be avoided under RCP 4.5 relative to RCP 8.5, at least through 2080; the ensemble means appear to be following divergent paths, however, such that it is possible a distinction could be made at some time after this point.

While the declines in global marine NPP over the next century are unequivocal, they manifest from diverse regional changes. Generally, tropical and subtropical NPP declines, whereas NPP increases at high latitudes over the 1920–2080 period (Figures 3b and 3c). The eastern equatorial Pacific and subarctic North Pacific shows NPP increases, while NPP declines over most of the Atlantic Ocean. The Southern Ocean mostly shows increases in NPP with some decreases along ~60°S. NPP in the Arctic Ocean, on the other hand, consistently increases in response to anthropogenic warming according these CESM simulations. As globally integrated marine NPP from individual ensembles over the 21st century overlap between emission scenarios due to natural variability among ensemble members (Figure 3a), it is difficult to see how a mitigation scenario would produce any avoidable impacts on a global scale. Therefore, in the following sections we divide marine NPP into its PFT components to examine phytoplankton regime shifts during the mid-21st century and divide the global ocean into various regions (primarily based on marine biomes) in order to explore the possibility of regional avoidable impacts for NPP in the ocean.

3.2. Shifts in Phytoplankton Assemblages

The CESM simulates three phytoplankton functional types, each of which shows a distinct globally integrated NPP trend (Figure 4). Diatom NPP remains fairly stable from 1920 to 2000, at which point it begins to decline (Figure 4a). The rate of diatom NPP decrease, which can be largely attributed to decreases in the North Atlantic (not shown), is less steep under the RCP 4.5 emission scenario (Figure 4a). In contrast, warming causes small

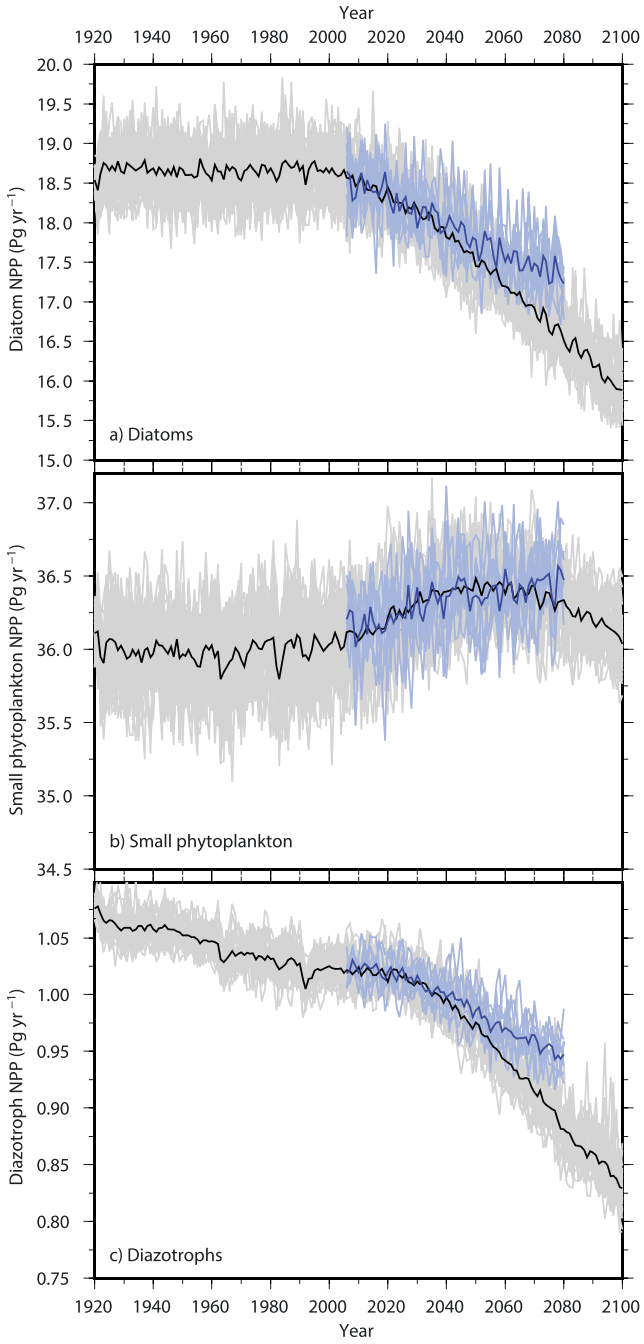

Figure 4. Global changes in marine NPP from 1920 to 2100 by each of the phytoplankton functional types in CESM: (a) diatoms, (b) small phytoplankton, and (c) diazotrophs. For the RCP 4.5 scenario, ensemble means are shown in blue and ensemble members are in light blue; for RCP 8.5, ensemble means are shown in black, with ensemble members in gray. Note the differences in *y* axis scales.

phytoplankton to expand into high latitudes resulting in an increase in NPP from this group during the first half of the 21st century (Figure 4b). NPP by small phytoplankton is reduced under RCP 8.5 after ~2050, however, due to severe nutrient limitation in the subtropics [*Moore et al.*, 2013]. Small phytoplankton NPP does not appear to show this decline under RCP 4.5, but it is possible such a decline manifests after 2080 (blue lines in Figure 4b). Diazotrophs, a minor contributor to total marine NPP, are confined to the warmer waters of the subtropics and tropics. This PFT, representing N-fixing phytoplankton, shows an initial slight decrease in NPP, followed by a steeper reduction after 2020 under RCP 8.5 from phosphorus and iron limitation (Figure 4c)

Table 1. Four Impact Types of Warming on NPP by the Two Main Phytoplankton Types in CESM[a]

	NPP Response	
Warming Impact Type	Diatoms	Small Phytoplankton
1	↑	↑
2	↓	↑
3	↑	↓
4	↓	↓

[a]Colors in the first column correspond to those in Figure 5.

[*Moore et al.*, 2013]. As diatoms and small phytoplankton account for most of marine NPP (~32% and ~66%, respectively), they also account for most of the natural variability, both showing between 1 and 1.5 Pg C yr^{-1} spread among ensemble members each year (Figure 4). Diazotroph NPP (~2% of total NPP), on the other hand, displays only a 0.05 Pg C yr^{-1} spread among ensemble members.

A further evaluation of NPP dynamics by the two main phytoplankton types (small phytoplankton and diatoms, responsible for ~98% of total marine NPP in CESM) offers lessons on the general impacts of warming on phytoplankton groups. Warming impacts these two groups differentially, resulting in four main impact types (Table 1): (1) NPP of both small phytoplankton and diatoms increases; (2) small phytoplankton NPP increases, diatom NPP decreases; (3) small phytoplankton NPP decreases, diatom NPP increases; or (4) NPP of both small phytoplankton and diatoms decreases. In terms of total NPP, impact type 1 indicates an increase in total NPP, while impact type 4 indicates a decrease; effects on total NPP are ambiguous for impact types 2 and 3. Nevertheless, these mid-21st century trends in phytoplankton NPP are important, as they indicate how warming is affecting phytoplankton communities in general, which can shape higher trophic levels in the marine food web [*Cheung et al.*, 2011; *Pörtner et al.*, 2014], as well as carbon export [*Moore et al.*, 2013; *Fu et al.*, 2016].

In Figure 5 we map these NPP impact types derived from long-term (ensemble mean) trends in small phytoplankton and diatoms from 2049 to 2080, under both RCP 4.5 and 8.5. Impact type 1 is found in the Southern Ocean and eastern equatorial Pacific, where both small phytoplankton and diatoms increase productivity. In the Southern Ocean, phytoplankton benefit from warming temperatures and declines in sea ice. Being generally high-macronutrient regions, phytoplankton in both the Southern Ocean and the eastern equatorial Pacific increase productivity due to increased lateral advection of iron from reduced upstream consumption [*Moore et al.*, 2013]. Impact type 1 is more expansive in the Arctic (north of the Pacific basin), eastern North Pacific, and in the South Atlantic with carbon emission mitigation (Figure 5a compared to 5b). Indeed, when nutrients become a limiting factor on NPP (with, e.g., more water column stratification from enhanced RCP 8.5 warming), then impact type 1 transitions to impact type 2: small phytoplankton NPP increases at the expense of diatom NPP (small phytoplankton are better competitors for nutrients) [*Moore et al.*, 2004]. Impact type 2 is seen extensively in the Arctic Ocean, subpolar regions, and in some areas of the Southern Ocean (Figure 5). Impact type 3 occurs mainly in the subpolar region of the Southern Ocean, where warming nutrient rich waters allow fast diatom growth rates (with increased lateral and vertical inputs of iron [*Moore et al.*, 2013]), thus outcompeting small phytoplankton. Impact type 3 arises in some patchy areas in the Southern Ocean under RCP 4.5, while stronger warming in the RCP 8.5 scenario induces a more cohesive band of impact type 3 in the subpolar Southern Ocean along ~60°S (Figure 5). Impact type 4 occurs under severe nutrient limitation and is widespread in the tropics and subtropics. While these impact types depict how 21st century warming may impact the dominant primary producers in marine ecosystems, changes in total NPP within marine biomes provide another mechanism to examine changes in an ecologically relevant context.

3.3. Long-Term Trends in Marine Biomes

Marine biomes partition the ocean into meaningful regions following natural biogeographical boundaries, which are primarily governed by large-scale ocean circulation. Changes in marine biomes from 1920 to 2080 are presented in the maps in Figures 6a–6c under both RCP 8.5 and 4.5, while global changes areal biome extent and productivity are presented in Figures 6d and 6e, respectively. Despite displaying the largest drops in productivity (Figures 3b, 3c, and 6e), equatorial biomes show little change in area (Figure 6d) mainly due to their being confined to a 5°N/S band around the equator [*Sarmiento et al.*, 2004], though we do observe a

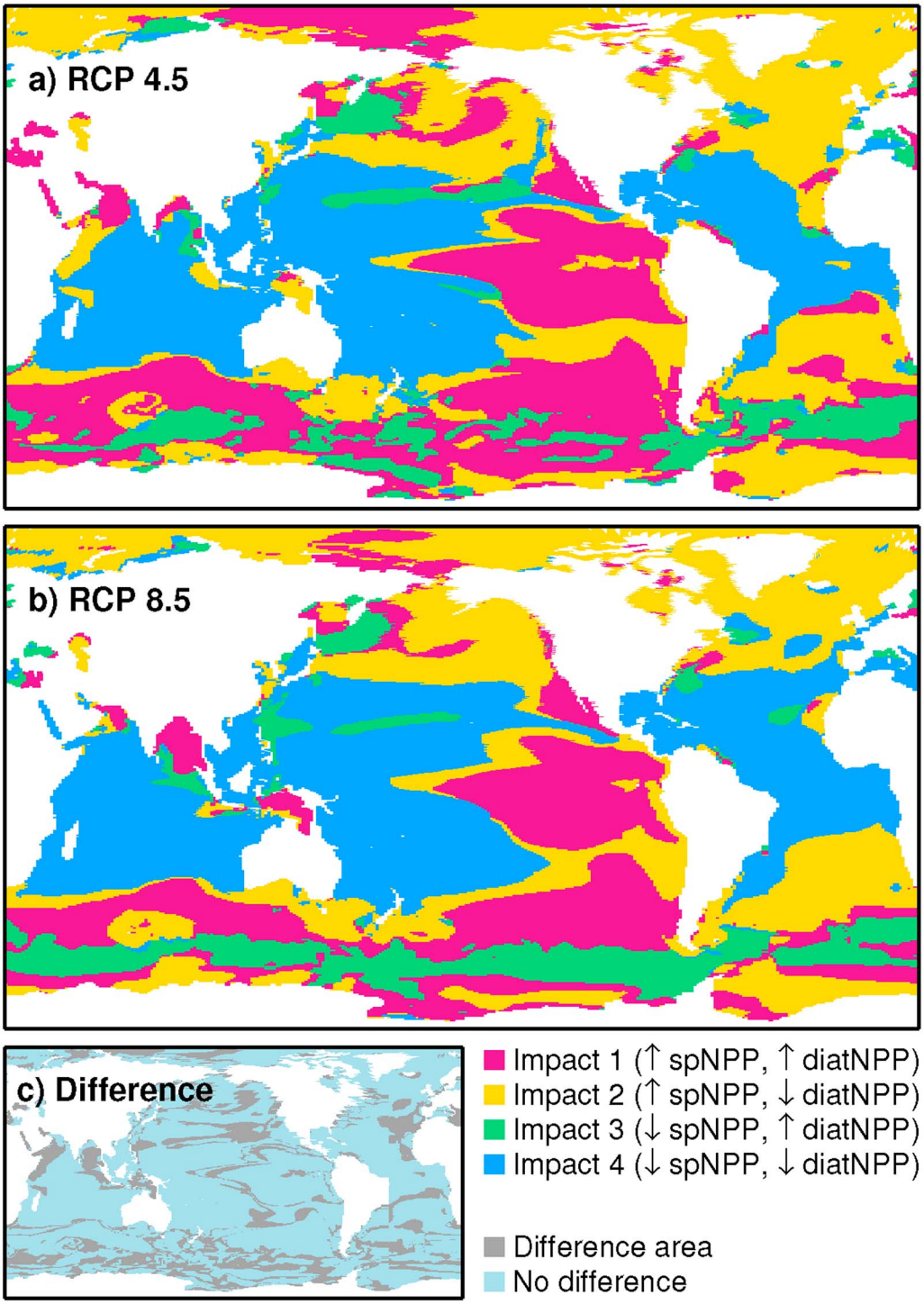

Figure 5. Map of four types of impacts (shown in Table 1) based on ensemble mean trends in NPP by small phytoplankton and diatoms from 2049 to 2080 for (a) RCP 4.5 and (b) RCP 8.5. All trends were categorized into impact types, regardless of magnitude. (c) A map of where the differences in Figures 5a and 5b are located. Statistically different trends between RCP scenarios are shown for regions listed Table 3.

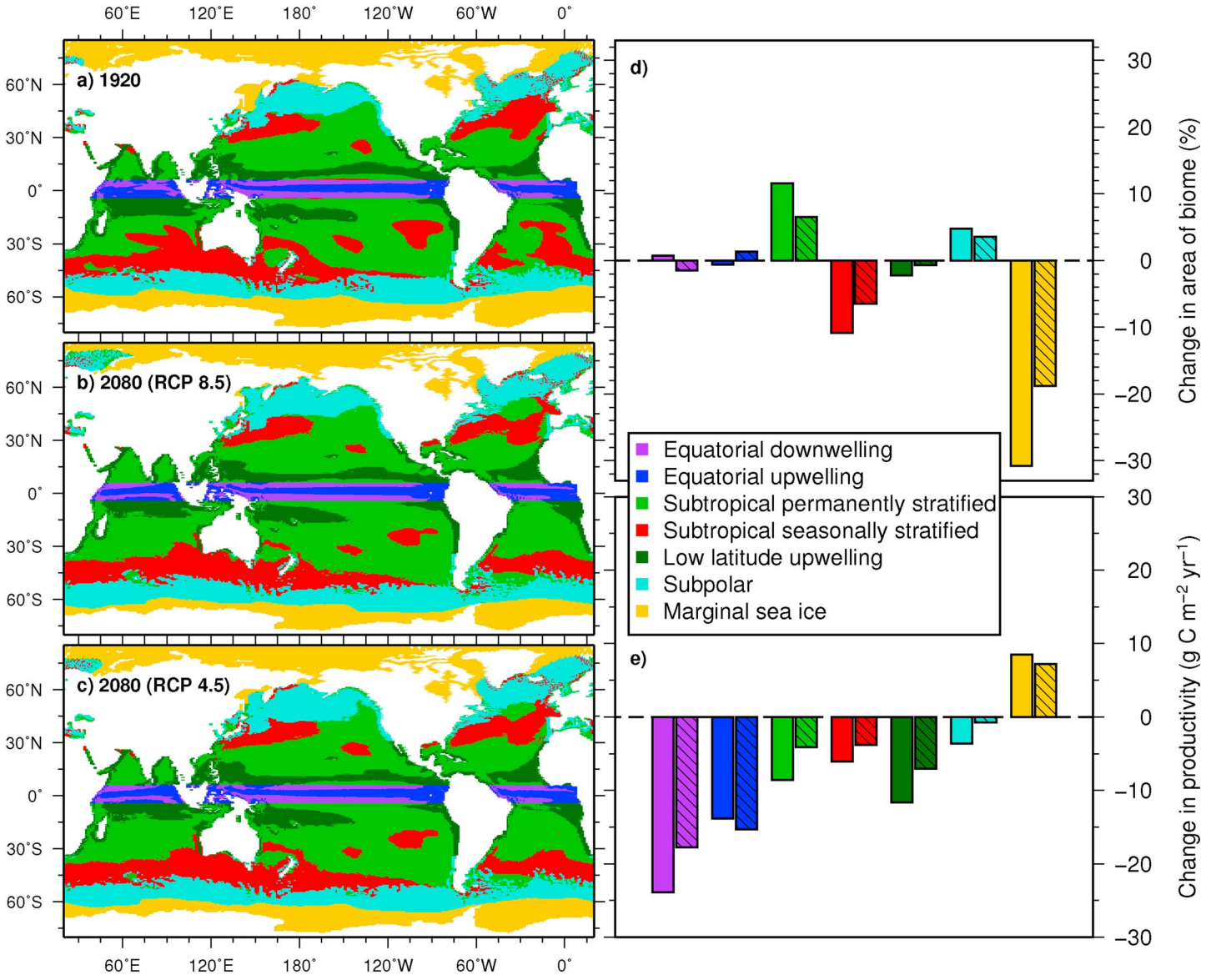

Figure 6. Changes in ensemble mean marine biomes from (a) 1920 to 2080 for (b) RCP 4.5 and (c) RCP 8.5. (d) Percent changes in biome area under both emission scenarios. (e) Changes in productivity within biomes. RCP 8.5 changes are shown in solid colors, and RCP 4.5 changes are hatched in Figures 6d and 6e. Marine biomes were calculated as in *Sarmiento et al.* [2004].

modification of upwelling/downwelling regions in the equatorial Indian Ocean with climate warming (Figures 6a–6c). The subtropical permanently stratified biome, however, expands under both warming scenarios, albeit to a substantially greater extent under RCP 8.5 ($>15 \times 10^6$ km^2, nearly a 12% increase compared to a 6.5% increase under RCP 4.5; Figure 6d). The enlargement of the subtropical permanently stratified biome is mainly at the expense of subtropical seasonally stratified and low-latitude upwelling biomes. The subpolar biome also expands as marginal sea ice areas (shown in yellow) disappear, gaining between 2 and 3×10^6 km^2 by 2080 (a 3% to 5% increase), depending on the emission scenario (Figure 6d). The subtropical seasonally stratified biome shows considerable reductions in area, as warming and stratification hinder deep winter mixing of the water. Low-latitude upwelling regions contract slightly due to water column stratification, but overall, we see the biggest declines in area in the marginal sea ice biome (−31% and −19% for RCP 8.5 and 4.5, respectively), as less sea ice is present in a warmer world.

All biomes, except the marginal sea ice biome, show a reduction in productivity per unit area (Figure 6e). The equatorial downwelling biome exhibits the largest declines in productivity of more than 20 g C m^{-2} yr^{-1} (−12%) from 1920 to 2080 if we follow RCP 8.5. The equatorial upwelling biome is the only one that shows a

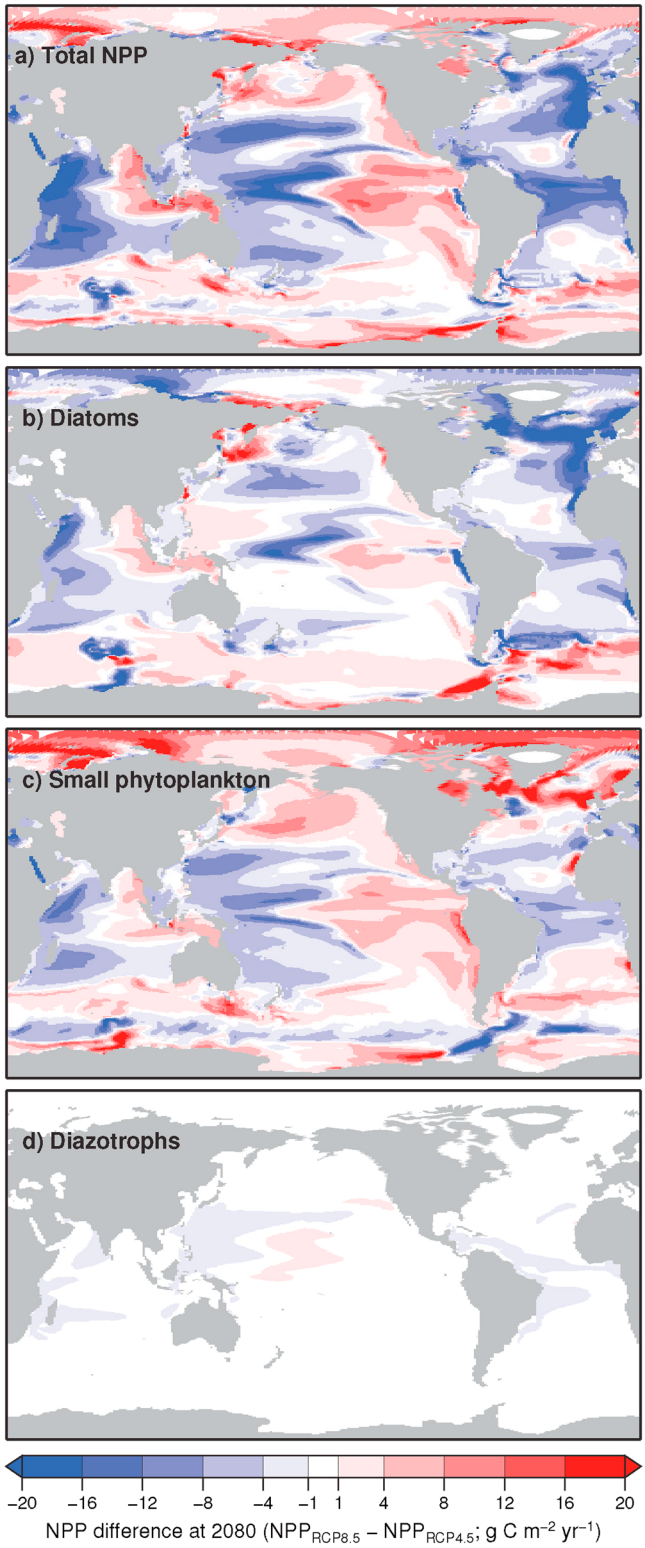

Figure 7. Long-term, forced avoidable impacts at 2080: the difference in the decadal averages (2071–2080) of ensemble means of vertically integrated NPP between RCP 8.5 and RCP 4.5 scenarios for (a) total NPP, (b) diatom NPP, (c) small phytoplankton NPP, and (d) diazotroph NPP.

Table 2. Ensemble Mean Trends in NPP From 2049 to 2080 in Each of the Seven Marine Biomes [*Sarmiento et al.*, 2004] ±1 Standard Deviation[a]

	NPP Trends in Marine Biomes, 2049–2080 (mg C m^{-2} yr^{-2})	
Biome	RCP 4.5	RCP 8.5
Eq-D	−10 ±15	−22 ±13
Eq-U	−2.7 ±10	−9.9 ±7.9
ST-PS	**−4.6 ±3.2**	**−13 ±3.3**
ST-SS	−0.094 ±1.9	−4.1 ±2.1
LL-U	−8.7 ±5.2	−19 ±4.9
SP	+2.4 ±2.7	−1.4 ±2.5
ICE	+7.8 ±3.7	+13 ±3.2

[a]The biome in bold shows significantly different NPP trends between emission scenarios. See section 2 for definition of biome abbreviations.

bigger decline under RCP 4.5, although the difference is not statistically significant. The only biome that does not show a reduction in its productivity by the end of the century is the marginal sea ice biome, showing an increase of between 7 and 8.5 g C m^{-2} yr^{-1} (a ∼10% increase). Light limitation of phytoplankton in these regions lessens with warming as the period of the year under ice coverage is reduced (Figure 6d). In Figures 5 and 6 we compare forced, long-term changes in marine NPP (using ensemble means eliminates most natural variability) under future emission scenarios, but which changes are actually avoidable if we follow RCP 4.5 rather than 8.5?

3.4. Avoidable Impacts in Marine Biomes and Major Basins

In Figure 7, we present differences in ensemble means at 2080 for total marine NPP and its PFT components between RCP 8.5 and 4.5, though, as discussed in the following paragraphs, these are not necessarily statistically avoidable. In terms of total NPP, the equatorial Pacific and high latitudes show a higher increase in NPP under RCP 8.5 versus RCP 4.5; the subtropics and the North Atlantic show a bigger decrease in NPP under RCP 8.5. As discussed above, the changes in total NPP are driven by changes in diatom and small phytoplankton NPP; diazotroph NPP is much smaller and shows smaller differences between the two forcing scenarios (Figures 7b–7d). In the far north, small phytoplankton NPP increases at the expense of diatom NPP (impact type 2), as described in Figure 5. Diatom NPP increases in the Southern Ocean (impact types 1 and 3 in Figures 5 and 7c). It is critical to consider whether the differences shown in Figure 7 (as well as in Figures 5 and 6) are statistically significant and thus avoidable, or attributable to the different forcing scenarios.

The CESM ensembles allow us to address the question of significance by quantifying the probability of trends in NPP under two scenarios. In Table 2, we present mean NPP trends in global marine biomes from 2049 to 2080 with standard deviation ($\pm 1\sigma$), calculated from the spread in trends among ensemble members. As each ensemble member comprises both natural variability and long-term trends in productivity, Table 2 shows how natural variability in trends over this period can impact realized long-term trends (i.e., whether a trend in biome productivity is actually significantly different between emission scenarios). Though all biomes (globally summed across basins) showed differing changes in NPP under the two emission scenarios, the only significant difference is for the subtropical permanently stratified biome (in bold in Table 2).

This concept is also illustrated using probability density function plots of trend magnitudes for major ocean regions (Figure 8). While the Pacific and Indian Oceans show differences in ensemble mean trends, these are not significantly different by the 1σ test, as there is substantial overlap in NPP trends among ensemble members from the two RCP scenarios. In the Southern Ocean all the ensemble member NPP trends (both emission scenarios) over the 2049 to 2080 period overlap. Therefore, NPP trends during the mid-21st century in the Pacific and Indian basins and the Southern Ocean are not statistically avoidable with RCP 4.5 relative to RCP 8.5. Conversely, in the Atlantic basin (Figure 8b) we see that the majority of ensemble member NPP trends do not overlap and there is a wide difference between ensemble means for the two forcing scenarios. Furthermore, the NPP trend ensemble means $\pm 1\sigma$ do not overlap for the Atlantic Ocean (although there is overlap for a 2σ test), and, therefore, we deem that there are significant warming impacts in the Atlantic that are avoidable.

We further divided up the ocean into 40 ecologically relevant regions based on hemisphere (N/S), major basin, and biome (see section 2). Out of 40 ocean regions, only 11 were deemed as having avoidable impacts.

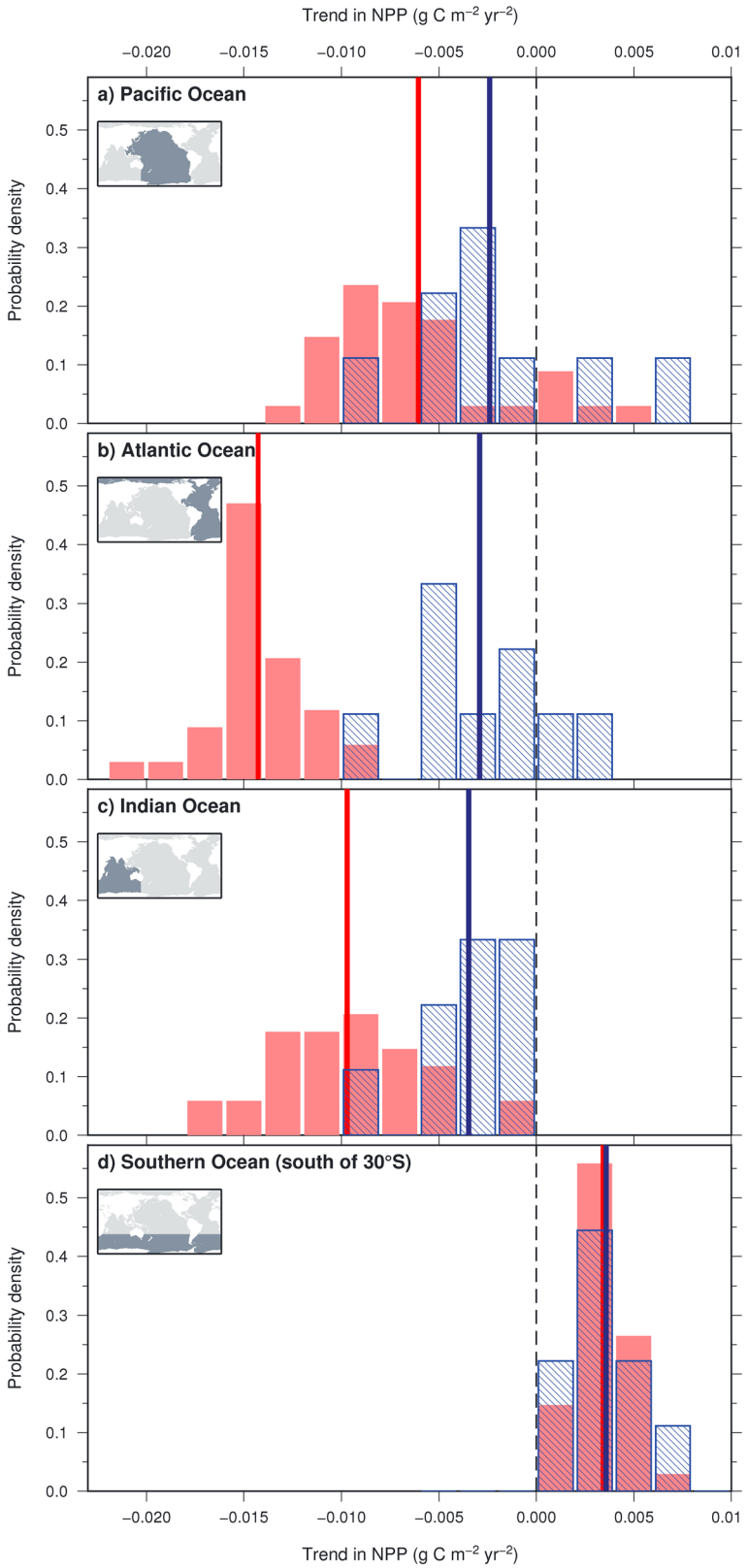

Figure 8. Probability density plots for trends in total NPP from 2049 to 2080 for the (a) Pacific Ocean, (b) Atlantic Ocean, (c) Indian Ocean, and (d) Southern Ocean based on trends observed in the CESM ensembles for the RCP 8.5 scenario (in red) and RCP 4.5 scenario (hatched blue bars) with ensemble means indicated by the solid colored lines. Masks for each region are shown in the small maps in the upper left corner of each plot.

Table 3. Regions Where Significant Impacts of Warming Are Avoidable Under RCP 4.5 With Ensemble Mean NPP Trends by the Two Main Phytoplankton Types Simulated in CESM[a]

Avoidable Impacts: NPP Trends in Main Phytoplankton Types, 2049–2080 (mg C m^{-2} yr^{-2})						
Region			RCP 4.5		RCP 8.5	
Basin	Zone	Biome	Small Phytoplankton	Diatoms	Small Phytoplankton	Diatoms
Indian	N	ST-PS	↑ +0.74	↑ +0.66	↓ −6.7	↓ −6.0
Pacific	S	ICE	↑ +2.9	↑ +2.6	↓ −7.0	↑ +9.0
Atlantic	Eq	Eq-D	↓ −7.5	↓ −6.4	↓ −22	↓ −19
Atlantic	Eq	Eq-U	↓ −4.8	↓ −8.2	↓ −18	↓ −23
Atlantic	N	ST-PS	↓ −2.4	↓ −6.3	↓ −9.1	↓ −11
Atlantic	N	ST-SS	↑ +11	↓ −20	↑ +3.4	↓ −35
Atlantic	N	LL-U	↓ −2.4	↓ −3.2	↓ −8.7	↓ −13
Atlantic	N	SP	↑ +22	↓ −33	↑ +31	↓ −63
Atlantic	S	ST-PS	↑ +0.52	↓ −1.4	↓ −2.5	↓ −8.5

[a]See section 2 for definition of biome abbreviations.

These "avoidable impact" regions based on total NPP are presented in Table 3 with N/S equatorial biomes grouped by upwelling and downwelling and classified as equatorial rather than by hemisphere (thus presented as only nine regions). Most of these avoidable impacts are in the Atlantic Ocean (Table 3 and Figure 9).

In Table 3 we further present trends in NPP between 2049 and 2080 by the two major phytoplankton groups for these avoidable impact regions, demonstrating what impact types (see above; Table 1) are avoidable. The only avoidable impact in the Indian basin is in the Northern Hemisphere subtropical permanently stratified biome, where under RCP 4.5, both small phytoplankton and diatom NPP are increasing (impact type 1; Tables 1 and 3). Following RCP 8.5, however, these trends for small phytoplankton and diatom NPP are entirely reversed over this period so that we observe impact type 4 (both major phytoplankton types decreasing) in the subtropical northern Indian Ocean. In this region, moderate RCP 4.5 warming results in increased

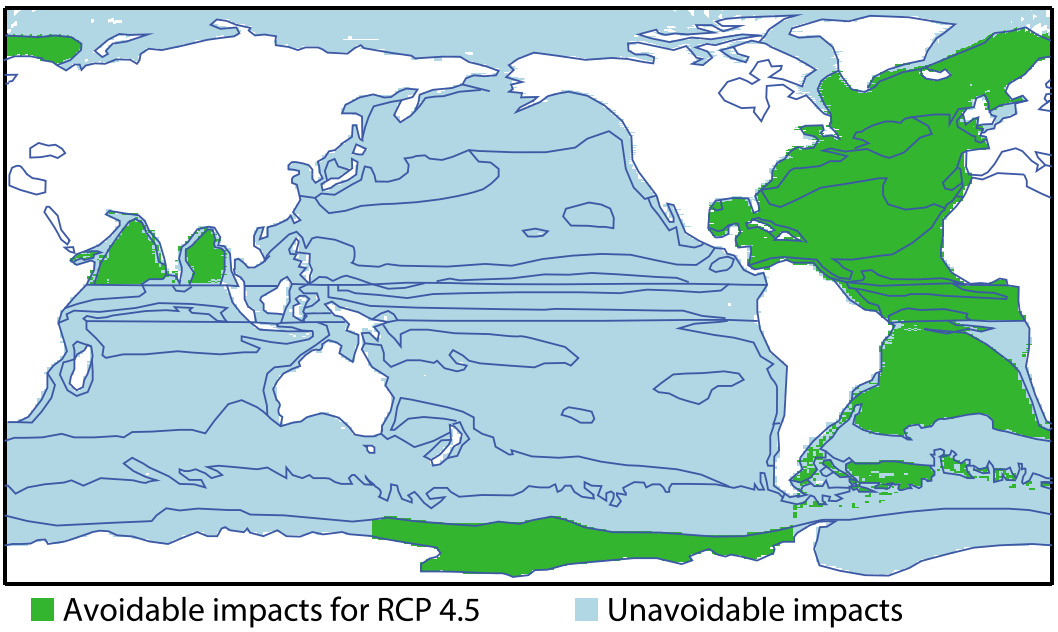

Figure 9. Regions with avoidable impacts in marine NPP, detected by no overlap of regional mean trends in NPP from 2049 to 2080 ± one standard deviation between ensemble simulations forced with RCP 4.5 and RCP 8.5 scenarios. Regions were constructed based on major basin, marine biomes, and N/S Hemisphere (see section 2). Biomes boundaries (from year 2049) are overlaid on the map.

phytoplankton growth rates, while more severe RCP 8.5 warming causes substantial shoaling of the mixed layer depth [*Moore et al.*, 2013] resulting in decreased nutrient availability and, thus, declines in production by both phytoplankton types. The Pacific basin also only contains one avoidable impact in the Southern Hemisphere marginal ice biome. Here we observe increasing NPP by both small phytoplankton and diatoms under both scenarios, albeit with significantly larger NPP trends observed for RCP 8.5 (Table 3). Atlantic equatorial and Northern Hemisphere subtropical permanently stratified and low-latitude upwelling biomes all show consistently decreasing NPP by both major phytoplankton types (impact type 4) regardless of scenario. Still, large NPP decreases are avoidable in these regions with mitigation (Table 3). In the North Atlantic subtropical seasonally stratified and subpolar biomes, however, we see increasing small phytoplankton NPP, while diatom NPP decreases (impact type 2). The opposing trends between the two major phytoplankton types are most pronounced in the subpolar biome. Lastly, the only Southern Hemisphere Atlantic biome to have an avoidable impact is the subtropical permanently stratified biome, where we see a reversal from a type 2 impact to a type 4 impact (changing from small phytoplankton NPP increasing/diatom NPP decreasing to NPP by both phytoplankton types decreasing; Table 3). There are no regions with avoidable impact type 3 (increasing diatom NPP, decreasing small phytoplankton NPP), as this impact type is mainly seen in the Southern Ocean where ensemble members from both scenarios overlap extensively (Figure 8d).

4. Discussion

In this study, we present an analysis of marine NPP as simulated by the CESM ensembles. By using ensembles of simulations, we were able to distinguish natural variability from forced trends. This is important, as marine NPP varies substantially from year-to-year due to natural climate variability (Figure 3a). The ensemble mean effectively removes natural variability, highlighting differences between long-term trends under a mitigation scenario and a high-emission scenario. However, some regions of the ocean display substantially more annual variability than others (Figure 1), and this needs to be considered when assessing whether or not a regional warming impact is indeed avoidable. In this section, we first examine long-term marine NPP trends in the context of total NPP, phytoplankton dynamics, and marine biomes. Next we discuss the important influence of natural variability when designating whether a warming impact is truly avoidable or not. This is followed by a discussion of the limitations of this study and future directions to advance modeling of phytoplankton production in the ocean. Lastly, we highlight broader implications and consequences of NPP changes with future anthropogenic warming, as projected by the CESM.

4.1. Long-Term Consequences of Anthropogenic Warming on Marine NPP

In this study, we assessed long-term trends in marine NPP, showing that according to these simulations, NPP in the ocean declines under both RCP 4.5 and RCP 8.5. On a global scale, the NPP declines under these forcing scenarios are not statistically different (Figure 3). However, distinctions between the two scenarios can be found by examining the changes on regional scales (based on major basins and marine biomes; Figures 6, 8, and 9 and Tables 2 and 3). As the ocean warms, changes in marine primary production will be a balance of direct effects of warming on physiology of plankton (both zooplankton and phytoplankton may show increased metabolic rates with warming) and indirect effects, such as stratification and subsequent nutrient limitation or altered light limitation [e.g., *Dutkiewicz et al.*, 2013; *Marinov et al.*, 2013]. Direct and indirect effects of sea surface warming may partially compensate for one another in terms of total NPP [*Laufkötter et al.*, 2015; *Marinov et al.*, 2013; *Dutkiewicz et al.*, 2013]. For example, increases in productivity in the marginal ice biome are countered by decreases within other biomes (Figure 6e). Warming increases the growth rates of phytoplankton and also increases stratification and inhibits deep mixing, resulting in nutrient limitation (for a detailed description of these warming effects on biogeochemistry in the Ross Sea see *Rickard and Behrens* [2016]). In line with this result, *Leung et al.* [2015] found latitudinally banded responses of phytoplankton to climate warming across CMIP5 models in the Southern Ocean: generally, phytoplankton abundance and production decreased in the subtropics, increased in a transitional band (~40–50°S), decreased in subpolar waters, and increased in the waters bordering Antarctica (see Figure 3). We also observe large increases in the subtropical permanently stratified biome (Figure 6d), and significantly stronger declines in productivity in this biome under RCP 8.5 than with the mitigation scenario (Table 2).

These regional biome changes lead to shifts in phytoplankton community structures (Figure 5). The effects of warming on phytoplankton communities can generally be characterized by the dynamics between two main phytoplankton groups: small phytoplankton and diatoms, referred to as "gleaners" (aka "K strategists")

and "opportunists" (aka "r strategists"), respectively, by *Dutkiewicz et al.* [2013]. These two groups of phytoplankton respond differentially to warming. As warming-induced stratification limits access to nutrients, it is generally expected that small phytoplankton will become increasingly dominant over larger ones, such as diatoms [see, e.g., *Morán et al.*, 2010; *Marinov et al.*, 2010]. Due to a larger surface area to volume ratio, small phytoplankton are more competitive for nutrients at low concentrations. This is parameterized in CESM in terms of half-saturation coefficients for nutrient uptake [see, e.g., *Marinov et al.*, 2010]. For example, small phytoplankton are 16 times more efficient at taking up PO_4 than diatoms at low PO_4 concentrations [*Moore et al.*, 2004]. Therefore, as the ocean warms and nutrients become scarcer, a shift to small phytoplankton-dominated ecosystems prevails (impact type 2; Table 1 and Figure 5). Recent increases in coccolithophores (small phytoplankton) in the North Atlantic indicate that we may already be observing a type 2 impact (increasing small phytoplankton NPP, while diatom NPP declines) [*Krumhardt et al.*, 2016; *Rivero-Calle et al.*, 2015]. However, natural climate variability (e.g., Atlantic Multidecadal Oscillation) [*Rivero-Calle et al.*, 2015] may play a significant role in these observations. Furthermore, both of these studies indicated that these pelagic calcifiers may be responding positively to increasing anthropogenic carbon in the upper mixed layer (not simulated in CESM), rather than increasing competition for nutrients.

Marinov et al. [2010] formulated a "critical nutrient hypothesis," which states that under (above) a certain threshold nutrient concentration, a nutrient change will influence small phytoplankton more (less) than diatoms. The geographical boundary of this threshold nutrient concentration is at ~45°N/S of latitude [*Marinov et al.*, 2010]. Although we see a similar boundary in terms of total NPP (see Figures 3b and 3c), we generally see latitudinally mixed NPP responses by diatoms and small phytoplankton over the latter 21st century when including all impacts of warming (i.e., changes in light and temperature, as well as nutrients; Figure 5). However, in agreement with *Marinov et al.* [2010], we observe substantial increases in diatom NPP in the Southern Ocean south of ~45°S, which can indeed be attributed to unused iron laterally advecting into this high-macronutrient region (from regions where productivity and, thus, nutrient usage has dropped) [*Moore et al.*, 2013]. In any case, based on the simulations presented here, avoidable impacts of anthropogenic warming at 2080 on diatom and small phytoplankton NPP are spatially diverse (Figures 7b and 7c).

4.2. Assessing Avoidable Impacts Using Ensemble Simulations

Our ability to discern differences in simulated NPP between two forcing scenarios depends on the sensitivity of NPP to warming (i.e., the magnitude of the forced trend) relative to the magnitude of natural variability. For instance, the equatorial Pacific shows stronger increases in the east and decreases in the west under RCP 8.5 than RCP 4.5 (Figures 3b, 3c, and 7), but due to high natural variability in this region (Figure 1c), these impacts cannot be deemed as avoidable. In other words, even though the difference between the NPP changes under the two forcings at 2080 is relatively high in magnitude (between −1 and −2 g C m^{-2} yr^{-1} in the west and +0.4 and +1.2 g C m^{-2} yr^{-1} in the east; Figure 7) they are not distinct between emission scenarios because the equatorial Pacific region displays such high natural variability. In contrast, negative trends in NPP in the Atlantic are stronger with more warming (>2 g C m^{-2} yr^{-1} difference between RCP 8.5 and 4.5; Figure 7), and, even given moderate variability (Figures 1c and 8b), the NPP trends in most areas of the Atlantic are significantly different between warming scenarios. Thus, we can distinguish a difference between the two forcing scenarios and classify some warming impacts in the Atlantic as avoidable (Figure 9). Here climate warming leads to a shallower mixed layer depth, decreased surface salinity, and increased stratification. These changes cause the deep convective mixing in the North Atlantic to weaken substantially under RCP 8.5 forcing [*Moore et al.*, 2013], a consistent result across CMIP5 models [*Stocker et al.*, 2013a], ultimately having negative impacts on primary production.

4.3. Limitations and Future Directions

A major limitation of this study is that the avoidable impacts are only assessed until year 2080, when the simulations with RCP 4.5 emissions ended. It is unknown if trends in global marine NPP assessed in this study will continue post-2080. Thus, we cannot distinguish whether the impacts discussed are truly avoidable beyond the latter 21st century. Adding to this uncertainty, *John et al.* [2015] suggest that after mitigation the ocean NPP may rebound and perhaps exceed preindustrial NPP. Furthermore, we are limited by the use of one Earth system model and therefore cannot address the role of structural uncertainty in NPP trends [*Frölicher et al.*, 2016; *Lovenduski et al.*, 2016].

Despite variations in drivers [*Laufkötter et al.*, 2015], all CMIP5 Earth system models predict future marine NPP decreases, though of varying magnitudes, with anthropogenic warming [*Cabré et al.*, 2015]. Even so,

simulation of physical ocean dynamics, model resolution, and parameterization of phytoplankton and zooplankton physiology can greatly influence the predictive effects of climate change on phytoplankton growth made by a model [*Cabré et al.*, 2015; *Laufkötter et al.*, 2015]. Earth system models have a limited number of PFTs, but reactions to warming by phytoplankton in reality may be more complex. For example, short life cycles of phytoplankton may allow for evolution and adaption of phytoplankton species to warming [e.g., *Schlüter et al.*, 2014]. Specifically, in CESM, the small phytoplankton PFT encompasses a large variety of species, which may have contrasting reactions to ocean warming [see, e.g., *Fu et al.*, 2007] or acidification [*Riebesell et al.*, 2000; *Iglesias-Rodriguez et al.*, 2008]. CESM, however, does not simulate the influence of changing carbonate chemistry on phytoplankton [*Moore et al.*, 2013]. As simulation of phytoplankton growth improves with future modifications to Earth system models (e.g., adding more PFTs), the predictive power of climate change impacts on marine primary production may become more robust.

4.4. Implications for Ecology and Export

This study offers motivation for both carbon emission mitigation and climate change adaptation policies. It is encouraging for mitigation efforts that much of the Atlantic Ocean contains anthropogenic warming NPP impacts that can be considered avoidable. Comprising the base of the marine food web, phytoplankton production changes could have cascading effects to living marine resources used by humans. Mitigation efforts may avoid a major drop in NPP in the Atlantic basin, a vital fishery region [*Food and Agriculture Organization*, 2011]. Even so, CESM simulates a shift toward small phytoplankton-dominated ecosystems in the North Atlantic under both emission scenarios (Figure 5 and Table 3); this alone could have important implications for marine ecosystems, for instance, reducing energy transferred to higher trophic levels (i.e., fish) [*Cheung et al.*, 2011].

However, the majority of ocean regions show that there is not a significant difference in 21st century marine NPP trends between a mitigation scenario and a business-as-usual scenario when taking natural variability into account (Figure 9). Furthermore, it appears unlikely that human societies will curb carbon emissions faster than indicated in the RCP 4.5 emission scenario. The emission reduction targets agreed upon at the 2015 Paris Climate Conference (COP21) would still result in roughly 2.7°C of warming, in line with projected warming under the RCP 4.5 scenario [*Stocker et al.*, 2013b]. Therefore, these simulations may offer motivation to focus adaptation efforts in regions where unavoidable impacts may negatively influence major fisheries (e.g., the low-latitude upwelling biome in the Indian Ocean; Figure 6). In addition to changes in living marine resources for human societies, warming impacts on marine NPP will also affect components of the global carbon cycle, such as carbon export to the deep sea.

Carbon export out of the euphotic zone to the deep ocean is strongly controlled by phytoplankton community structure, with diatoms generally being more efficient exporters than small phytoplankton [*Moore et al.*, 2013]. The decrease in diatom NPP by 2080 (~7% for RCP 4.5 and ~12% for RCP 8.5), therefore, coincides with decreased export (not shown) [see *Moore et al.*, 2013]. A decrease in export production with warming is a consistent result among CMIP5 models [*Cabré et al.*, 2015], though *Laufkötter et al.* [2016] showed that substantial variation exists among models for the drivers of this decrease (e.g., particle formation/remineralization versus changes in ecosystem structure). Some studies indicate that phytoplankton-type contribution to export is proportional to their contribution to total NPP, by way of aggregation and zooplankton grazing, rather than being dependent on phytoplankton size [*Richardson and Jackson*, 2007]. Yet even in this case, we would still expect a long-term decrease in organic carbon export as total marine NPP is reduced on average by ~2% for RCP 4.5 and ~4% for RCP 8.5 by 2080.

5. Conclusion

In this study, we use CESM ensemble simulations to show where anthropogenic warming impacts on marine NPP are avoidable following the forcing scenario RCP 4.5. Ensembles of simulations allow for the quantification of internal variability of marine NPP, which facilitates the statistical comparison between two RCP emission scenarios. Small phytoplankton and diatoms are responsible for most of the primary production in CESM simulations—warming impacts on NPP can be categorized based on dynamics in carbon fixation by these two groups. These ensemble simulations suggest significantly higher expansion of, and productivity drops within, the subtropical permanently stratified biome under the RCP 8.5 emission scenario. In general, we find more avoidable impacts in the Atlantic basin than in other oceanic regions, as drops in productivity observed in the Atlantic are significantly less following RCP 4.5 in lieu of RCP 8.5.

Acknowledgments
CESM ensemble output is available from the Earth System Grid (https://www.earthsystemgrid.org/dataset/ucar.cgd.ccsm4.CESMCAM5BGCLE.html and https://www.earthsystemgrid.org/dataset/ucar.cgd.ccsm4.CESMCAM5BGCME.html). CESM computing resources were provided by CISL at NCAR. We thank Oregon State University for the satellite-derived NPP data (https://www.science.oregonstate.edu/ocean.productivity/). We also thank BATS (https://bats.bios.edu) and HOT (https://hahana.soest.hawaii.edu/hot/) research teams for their sustained efforts collecting oceanographic data. Funding for this research was provided by NSF (OCE-1558225, OCE-1258995, and OCE-1155240), and NOAA (NA12OAR4310058). The National Center for Atmospheric Research is funded by the National Science Foundation.

References

Behrenfeld, M. J., and P. G. Falkowski (1997), Photosynthetic rates derived from satellite-based chlorophyll concentration, *Limnol. Oceanogr.*, *42*(1), 1–20, doi:10.4319/lo.1997.42.1.0001.

Bopp, L., et al. (2013), Multiple stressors of ocean ecosystems in the 21st century: Projections with CMIP5 models, *Biogeosciences*, *10*(10), 6225–6245, doi:10.5194/bg-10-6225-2013.

Cabré, A., I. Marinov, and S. Leung (2015), Consistent global responses of marine ecosystems to future climate change across the IPCC AR5 Earth system models, *Clim. Dyn.*, *45*(5-6), 1253–1280, doi:10.1007/s00382-014-2374-3.

Cheung, W. W. L., V. W. Y. Lam, J. L. Sarmiento, K. Kearney, R. Watson, D. Zeller, and D. Pauly (2010), Large-scale redistribution of maximum fisheries catch potential in the global ocean under climate change, *Global Change Biol.*, *16*(1), 24–35, doi:10.1111/j.1365-2486.2009.01995.x.

Cheung, W. W. L., J. Dunne, J. L. Sarmiento, and D. Pauly (2011), Integrating ecophysiology and plankton dynamics into projected maximum fisheries catch potential under climate change in the Northeast Atlantic, *ICES ICES J. Mar. Sci.: J. du Conseil*, *68*(6), 1008–1018, doi:10.1093/icesjms/fsr012.

Deser, C., R. Knutti, S. Solomon, and A. S. Phillips (2012), Communication of the role of natural variability in future North American climate, *Nature Clim. Change*, *2*(11), 775–779.

Dutkiewicz, S., J. R. Scott, and M. J. Follows (2013), Winners and losers: Ecological and biogeochemical changes in a warming ocean, *Global Biogeochem. Cycles*, *27*(2), 463–477, doi:10.1002/gbc.20042.

Falkowski, P. (2012), Ocean science: The power of plankton, *Nature*, *483*(7387), S17—S20.

Food and Agriculture Organization (2011), *Review of the State of World Marine Fishery Resources*, 334 pp., Food and Agriculture Organization of the United Nations, Rome.

Frölicher, T. L., F. Joos, G.-K. Plattner, M. Steinacher, and S. C. Doney (2009), Natural variability and anthropogenic trends in oceanic oxygen in a coupled carbon cycle–climate model ensemble, *Global Biogeochem. Cycles*, *23*, GB1003, doi:10.1029/2008GB003316.

Frölicher, T. L., K. B. Rodgers, C. A. Stock, and W. W. L. Cheung (2016), Sources of uncertainties in 21st century projections of potential ocean ecosystem stressors, *Global Biogeochem. Cycles*, *30*, 1224–1243, doi:10.1002/2015GB005338.

Fu, F.-X., M. E. Warner, Y. Zhang, Y. Feng, and D. A. Hutchins (2007), Effects of increased temperature and CO_2 on photosynthesis, growth, and elemental ratios in marine Synechococcus and Prochlorococcus (cyanobacteria), *J. Phycol.*, *43*(3), 485–496, doi:10.1111/j.1529-8817.2007.00355.x.

Fu, W., J. T. Randerson, and J. K. Moore (2016), Climate change impacts on net primary production (NPP) and export production (EP) regulated by increasing stratification and phytoplankton community structure in the CMIP5 models, *Biogeosciences*, *13*(18), 5151–5170, doi:10.5194/bg-13-5151-2016.

Hawkins, E., and R. Sutton (2009), The potential to narrow uncertainty in regional climate predictions, *Bull. Am. Meteorol. Soc.*, *90*(8), 1095–1107, doi:10.1175/2009BAMS2607.1.

Henson, S. A., C. Beaulieu, and R. Lampitt (2016), Observing climate change trends in ocean biogeochemistry: When and where, *Global Change Biol.*, *22*(4), 1561–1571, doi:10.1111/gcb.13152.

Iglesias-Rodriguez, M. D., et al. (2008), Phytoplankton calcification in a high-CO_2 world, *Science*, *320*(5874), 336–340, doi:10.1126/science.1154122.

John, J. G., C. A. Stock, and J. P. Dunne (2015), A more productive, but different, ocean after mitigation, *Geophys. Res. Lett.*, *42*(22), 9836–9845, doi:10.1002/2015GL066160.

Kay, J. E., et al. (2015), The Community Earth System Model (CESM) large ensemble project: A community resource for studying climate change in the presence of internal climate variability, *Bull. Am. Meteorol. Soc.*, *96*(8), 1333–1349, doi:10.1175/BAMS-D-13-00255.1.

Krumhardt, K. M., N. S. Lovenduski, N. M. Freeman, and N. R. Bates (2016), Apparent increase in coccolithophore abundance in the subtropical North Atlantic from 1990 to 2014, *Biogeosciences*, *13*(4), 1163–1177, doi:10.5194/bg-13-1163-2016.

Laufkötter, C., et al. (2015), Drivers and uncertainties of future global marine primary production in marine ecosystem models, *Biogeosciences*, *12*(23), 6955–6984, doi:10.5194/bg-12-6955-2015.

Laufkötter, C., et al. (2016), Projected decreases in future marine export production: the role of the carbon flux through the upper ocean ecosystem, *Biogeosciences*, *13*(13), 4023–4047, doi:10.5194/bg-13-4023-2016.

Leung, S., A. Cabré, and I. Marinov (2015), A latitudinally banded phytoplankton response to 21st century climate change in the Southern Ocean across the CMIP5 model suite, *Biogeosciences*, *12*(19), 5715–5734, doi:10.5194/bg-12-5715-2015.

Levis, S., A. Badger, B. Drewniak, C. Nevison, and X. Ren (2016), CLMcrop yields and water requirements: Avoided impacts by choosing RCP 4.5 over 8.5, *Clim. Change*, 1–15, doi:10.1007/s10584-016-1654-9.

Long, M. C., K. Lindsay, S. Peacock, J. K. Moore, and S. C. Doney (2013), Twentieth-century oceanic carbon uptake and storage in CESM1(BGC), *J. Clim.*, *26*(18), 6775–6800, doi:10.1175/JCLI-D-12-00184.1.

Long, M. C., C. Deutsch, and T. Ito (2016), Finding forced trends in oceanic oxygen, *Global Biogeochem. Cycles*, *30*, 381–397, doi:10.1002/2015GB005310.

Lovenduski, N. S., G. A. McKinley, A. R. Fay, K. Lindsay, and M. C. Long (2016), Partitioning uncertainty in ocean carbon uptake projections: Internal variability, emission scenario, and model structure, *Global Biogeochem. Cycles*, *30*, 1276–1287, doi:10.1002/2016GB005426.

Marinov, I., S. C. Doney, and I. D. Lima (2010), Response of ocean phytoplankton community structure to climate change over the 21st century: Partitioning the effects of nutrients, temperature and light, *Biogeosciences*, *7*(12), 3941–3959, doi:10.5194/bg-7-3941-2010.

Marinov, I., S. C. Doney, I. D. Lima, K. Lindsay, J. K. Moore, and N. Mahowald (2013), North-south asymmetry in the modeled phytoplankton community response to climate change over the 21st century, *Global Biogeochem. Cycles*, *27*, 1274–1290, doi:10.1002/2013GB004599.

McKinley, G. A., D. J. Pilcher, A. R. Fay, K. Lindsay, M. C. Long, and N. S. Lovenduski (2016), Timescales for detection of trends in the ocean carbon sink, *Nature*, *530*(7591), 469–472.

Moore, J. K., S. C. Doney, and K. Lindsay (2004), Upper ocean ecosystem dynamics and iron cycling in a global three-dimensional model, *Global Biogeochem. Cycles*, *18*, GB4028, doi:10.1029/2004GB002220.

Moore, J. K., K. Lindsay, S. C. Doney, M. C. Long, and K. Misumi (2013), Marine ecosystem dynamics and biogeochemical cycling in the Community Earth System Model [CESM1(BGC)]: Comparison of the 1990s with the 2090s under the RCP4.5 and RCP8.5 scenarios, *J. Clim.*, *26*(23), 9291–9312, doi:10.1175/JCLI-D-12-00566.1.

Morán, X. A. G., A. López-Urrutia, A. Calo-Díaz, and W. K. W. Li (2010), Increasing importance of small phytoplankton in a warmer ocean, *Global Change Biol.*, *16*(3), 1137–1144, doi:10.1111/j.1365-2486.2009.01960.x.

Pörtner, H.-O., D. Karl, P. Boyd, W. Cheung, S. Lluch-Cota, Y. Nojiri, D. Schmidt, and P. Zavialov (2014), Climate change 2014: Impacts, adaptation, and vulnerability. Part A: Global and sectoral aspects, in *Contribution of Working Group II to the Fifth Assessment Report of the Intergovernmental Panel on Climate Change: Ocean Systems*, pp. 411–484, Cambridge Univ. Press, Cambridge, U. K., and New York.

Richardson, T. L., and G. A. Jackson (2007), Small phytoplankton and carbon export from the surface ocean, *Science*, *315*(5813), 838–840, doi:10.1126/science.1133471.

Rickard, G., and E. Behrens (2016), CMIP5 Earth system models with biogeochemistry: A Ross Sea assessment, *Antarct. Sci.*, *28*(5), 327–346, doi:10.1017/S0954102016000122.

Riebesell, U., I. Zondervan, B. Rost, P. D. Tortell, R. E. Zeebe, and F. M. M. Morel (2000), Reduced calcification of marine plankton in response to increased atmospheric CO_2, *Nature*, *407*(6802), 364–367.

Rivero-Calle, S., A. Gnanadesikan, C. E. Del Castillo, W. M. Balch, and S. D. Guikema (2015), Multidecadal increase in North Atlantic coccolithophores and the potential role of rising CO_2, *Science*, *350*(6267), 1533–1537, doi:10.1126/science.aaa8026.

Rodgers, K. B., J. Lin, and T. L. Frölicher (2015), Emergence of multiple ocean ecosystem drivers in a large ensemble suite with an Earth system model, *Biogeosciences*, *12*(11), 3301–3320, doi:10.5194/bg-12-3301-2015.

Sanderson, B. M., K. W. Oleson, W. G. Strand, F. Lehner, and B. C. O'Neill (2015), A new ensemble of GCM simulations to assess avoided impacts in a climate mitigation scenario, *Clim. Change*, 1–16, doi:10.1007/s10584-015-1567-z.

Sarmiento, J. L., et al. (2004), Response of ocean ecosystems to climate warming, *Global Biogeochem. Cycles*, *18*, GB3003, doi:10.1029/2003GB002134.

Schlüter, L., K. T. Lohbeck, M. A. Gutowska, J. P. Groger, U. Riebesell, and T. B. H. Reusch (2014), Adaptation of a globally important coccolithophore to ocean warming and acidification, *Nature Clim. Change*, *4*(11), 1024–1030.

Stocker, T., et al. (2013a), Climate Change 2013: The Physical Science Basis, in *Contribution of Working Group I to the Fifth Assessment Report of the Intergovernmental Panel on Climate Change*, chap. Technical Summary, pp. 1535, Cambridge Univ. Press, Cambridge, U. K., and New York., doi:10.1017/CBO9781107415324.

Stocker, T., D. Qin, G.-K. Plattner, M. Tignor, S. Allen, J. Boschung, A. Nauels, Y. Xia, V. Bex, and P. Midgley (2013b), Climate change 2013: The physical science basis, in *Contribution of Working Group I to the Fifth Assessment Report of the Intergovernmental Panel on Climate Change Chap. IPCC, 2013: Summary for Policymakers*, pp. 1535, Cambridge Univ. Press, Cambridge, U. K., and New York., doi:10.1017/CBO9781107415324.

Tebaldi, C., and M. F. Wehner (2016), Benefits of mitigation for future heat extremes under RCP4.5 compared to RCP8.5, *Clim. Change*, 1–13, doi:10.1007/s10584-016-1605-5.